ISTANBUL UNIVERSITY PRESS

RESEARCH ARTICLE

Eur J Biol

The Effects of SARS CoV-2 nsp13 Mutations on the Structure and Stability of Helicase in Chinese Isolates

Ekrem Akbulut[1]

[1]Malatya Turgut Özal University, Department of Bioengineering, Malatya, Turkiye

ORCID IDs of the authors: E.A. 0000-0002-7526-9835

Please cite this article as: Akbulut E. The Effects of SARS CoV-2 nsp13 Mutations on the Structure and Stability of Helicase in Chinese Isolates. Eur J Biol. Advanced online publication. DOI: 10.26650/EurJBiol.2022.1061858

ABSTRACT

Objective: Coronavirus Disease 2019 (COVID19) is a viral disease caused by Severe Acute Respiratory Syndrome Coronavirus-2 (SARS CoV-2). The high mutation propensity of the SARS CoV-2 genome is one of the biggest threats to the long-term validity of treatment options. Helicases are anti-viral targets because of the vital role they play in the viral life cycle. In this study, changes in the protein structure caused by SARS CoV-2 nsp13 mutations were investigated to contribute to the development of effective antiviral drugs.

Materials and Methods: Genome data of 298 individuals located in the China location were examined. The mutant model was built using deep learning algorithms. Model quality assessment was done with QMEAN. Protein stability analyses were performed with DynaMut2 and Cutoff Scanning Matrix stability. Changes in substrate affinity were performed with Haddock v2.4.

Results: In this study, twenty-eight mutations in nsp13 were identified (23 sense, 5 missense). The changes in protein structure caused by the five missense mutations (Leu14Phe, Arg15Ser, Arg21Ser, Leu235Phe, Ala454Thr) were modeled. The mutations caused a decrease in the stability of SARS CoV-2 helicase (-0.99, -1.66, -1.15, -0.54, and -0.73 for Leu14Phe, Arg15Ser, Arg21Ser, Leu235Phe, Ala454Thr, respectively). The mutations reduced the helicase's affinity to the substrate. The docking scores for wild-type and mutant helicase were -84.4±1.4 kcal.mol^{-1} and -71.1±6.7 kcal.mol^{-1}, respectively.

Conclusion: Helicase mutations caused a decrease in the protein stability and nucleic acid affinity of the SARS CoV-2 helicase. The results provide important data on the development of potential antivirals and the effect of mutation on the functions of viral proteins.

Keywords: COVID19, helicase, mutation, protein stability, SARS CoV-2 genome, substrate affinity

INTRODUCTION

The Corona Virus Disease 2019 (COVID-19) is characterized by a variety of clinical features ranging from asymptomatic acute respiratory distress to multi-organ dysfunction (1,2). The SARS CoV-2, which has a high risk of transmission and death rate, caused 289 million people to become ill and 5.44 million people to die in the last two years (3). The etiological agent of COVID-19, the SARS CoV-2 virus is positive polarity, single-strand RNA virus with a genome of 29.9 kb (4). The SARS CoV-2 genome consists of two overlapping open reading frames (ORF1ab and ORF1a), four structural proteins (spike, envelope, nucleocapsid, membrane) and six accessory proteins (ORF3a, ORF6, ORF7a, ORF7b, ORF8 and ORF10) (5). Open reading frames are involved in the continuous synthesis of 16 non-structural proteins (nsps) that play important roles in the viral life cycle (6). SARS CoV-2 helicase (non-structural protein 13/nsp13) catalyzes a 5′–3′ direction unwinding process in the presence of nucleotide three phosphate to transform duplex oligonucleotides (RNA or DNA) into single strands. Helicase, which is essential for the life cycle of the virus, is one of the important structural targets for therapeutic agents

Corresponding Author: Ekrem Akbulut E-mail: ekremakbulut@gmail.com

Submitted: 23.01.2022 • **Revision Requested:** 17.02.2022 • **Last Revision Received:** 19.02.2022 • **Accepted:** 21.03.2022 • **Published Online:** 13.04.2022

(7,8). Helicase plays an active role in the replication process of the SARS CoV-2 in the host together with RNA-dependent RNA polymerase. Helicases have additional biological roles such as transcription, mRNA splicing, mRNA export, RNA stability, translation, mitochondrial gene expression, and nucleic acid packaging into virions (9). The high mutation risk of the SARS CoV-2 genome, like with other RNA viruses, poses a major threat to the validity of therapeutic options. Modeling changes induced by mutations in the viral proteome supports the development of potent antivirals (10-12).

The changes in the helicase structure caused by nsp13 mutations of SARS CoV-2 were investigated to develop robust and valid therapeutics, in this study.

MATERIAL AND METHODS

Sequence Data and Mutation Analysis

The genome sequence data for the samples were obtained from the NCBI Virus database. The genome data of 12,218 individuals located on the Asian continent were examined and the sequence data from 298 individuals from the China location was used for analysis in this study. Reference sequence data for the genome and protein was used NC_045512.2 and YP_009725308.1, respectively (4). The sequence data was aligned with the MAFFT (v7.490) multiple sequence alignment program FFT-NS-i algorithm (13). The scoring matrix BLOSUM 80, and 1 PAM was chosen for the amino acid sequences, and nucleotide, respectively (14,15). The gap opening penalty was used as 2.0. The mutated residues were analyzed MegaX (16).

Tertiary Structure of Mutant Protein and Protein Stability Analysis

The tertiary structure of mutant nsp13 was generated by the method of homology modeling using RoseTTAFold (17). The 7NIO (pdb accession code) was selected as a template (18). The QMEAN was used for structural validation and model of mutant nsp13 (19). Superimpose and conformational analyses of the wild-type and mutant helicase were performed with the PyMOL (ver2.4.1) and NGL viewer (20). Topological differences of wild-type and mutant nsp13 proteins were calculated with the i-Tasser TM-Score and root mean square deviation (RMSD) algorithm (21). An analysis of changes in protein stability was performed using the DynaMut2 and mutation Cutoff Scanning Matrix (mCSM) (22,23). The mCSM provides graph-based structural signatures, which is used to examine the effect of mutations on protein stability and interaction. The mCSM, extending the inter-residual signature to an atomic level, is a protein structural tool used for large-scale protein function prediction and structural classification. The mCSM workflow consists of: collection and preprocessing of thermodynamic and structural data, extraction of residue environments, signature calculation and noise reduction, supervised learning, and mutation effect estimation and validation (24,25). Another approach used to analyze missense mutations' impact on protein stability was DynaMut2, which uses protein dynamics, wild-type residue environment, substitution trends and contact potential scores, and interatomic distance data to train and test machine learning algorithms (22). Non-covalent molecular interactions were calculated using Arpeggio (26).

Docking

The change in helicase – nucleic acid affinity after the mutation was evaluated using the Haddock version 2.4 (27). The active site for the helicase were residues number 288, 289, 290, 320, 374, 375, 404, 442, 443, 540, 567. A number of structures for rigid body docking was set to 1000. A number of trials for rigid body minimization was set to 5. A number of structures for semi-flexible refinement was set to 200. Refined with short molecular dynamics in open solvent using water. The clustering method was selected Fraction of Common Contacts (FCC). The RMSD cutoff for clustering was set to 0.6 Å. The Kyte-Doolittle hydrophobicity scale method was used for solvating. A cutoff distance (proton-acceptor) to define a hydrogen bond was set to 2.5 Å. A cutoff distance (carbon-carbon) to define a hydrophobic contact was set to 3.9 Å. The docking results were visualized with Discovery SV (ver20.1, DDS Biovia).

RESULTS

A mutation analysis revealed that there were 23 sense and 5 missense (Leu14Phe, Arg15Ser, Arg21Ser, Leu235Phe, and Ala454Thr) mutations in the helicase of SARS CoV-2 from Chinese isolates (Table 1). The mutant nsp13 protein was modeled using the deep learning-based modeling approach, RoseTTAFold. The Tm-score was 0.9787. The mutations caused changes in protein conformation and topological structure (rmsd 0.325 Å) (Figure 1). The five mutations causing amino acid changes showed a destabilizing effect in the helicase structure (-0.99, -1.66, -1.15, -0.54, and -0.73 kcal.mol^{-1} respectively). The mutations changed the bond conformation between the residues, forming the tertiary structure (Figure 2). After the Leu14Phe mutation, two interactions (Phe14-Cys26 and Phe14-Cys27) that were not in the wild-type appeared in the tertiary structure of the mutant helicase (Figures 2a and b). Increased inter-residual bond interaction may limit the movement of the helicase N-terminal domain. The Arg15Ser mutation reduced the local tertiary conformation provided by seven hydrophobic, nine polar, and one Van der Walls interactions in the wild protein to four polar and one hydrogen bond in the mutant protein (Figures 2c and d). The Arg21Ser mutation revealed the most striking reduction in terms of tertiary structure bond formation. The wild-type helicase, which demonstrated nine different interactions with five amino acids at position twenty-one, made single amino acid and single bond interaction in the mutant protein (Figures 2e and f). Although the Leu235Phe mutation abolished the hydrogen bonds between 235-Leu132 and 235-Ser385, it revealed an increase in polar and hydrophobic interactions (Figures 2g and h). The Ala454Thr mutation introduced an additional Asn459 polar interaction, which was not in wild-type (Figures 2i and j).

Table 1. SARS CoV-2 helicase mutations in Chinese isolates.

Genomic Location	Codon Change	Mutation	Sense/Missense
16255	GTA > GTT	Val6Val	sense
16279	TTT > TTA	Leu14Phe	missense
16280	CGA > AGA	Arg15Arg	sense
16282	AGT > AGA	Arg15Ser	missense
16297	ATT > ATA	Ile20Ile	sense
16298	AGT > CGT	Arg21Ser	missense
16300	CGG > CGT	Arg21Arg	sense
16342	ATT > ATA	Ile35Ile	sense
16364	CTG > TTG	Leu43Leu	sense
16420	ACA > ACT	Thr61Thr	sense
16450	TAC > TAT	Tyr71Tyr	sense
16498	GGT > GGA	Gly87Gly	sense
16567	GCT > GCA	Ala110Ala	sense
16601	CTA > TTA	Leu122Leu	sense
16762	CCT > CCA	Pro175Pro	sense
16769	AGA > CGA	Arg178Arg	sense
16879	ACT > ACA	Thr214Thr	sense
16894	TTG > TTA	Leu219Leu	sense
16921	ACC > ACA	Thr228Thr	sense
16942	TTT > TTA	Leu235Phe	missense
16978	GTG > GTT	Val247Val	sense
17377	ACT > ACA	Thr380Thr	sense
17416	GCA > GCT	Ala393Ala	sense
17530	ACA > ACT	Thr431Thr	sense
17597	ACT > GCT	Ala454Thr	missense
17990	CTG > TTG	Leu585Leu	sense
18020	CGG > AGG	Arg595Arg	sense
18031	GCT > GCA	Ala598Ala	sense

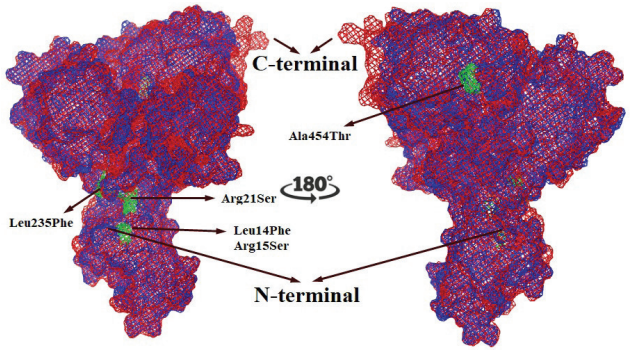

Figure 1. Display of changes caused by mutations in helicase in superimpose mode blue: wild-type helicase, red: mutant helicase, green: mutant residues

The mutations caused a decrease in the nucleic acid affinity of helicase (lowest ΔΔG -84.4±1.4 kcal.mol^{-1} and -71.1±6.7 kcal.mol^{-1} for wild-type and mutant, respectively) (Table 2). The Z-scores suggested that the mutant docking pattern was more accurate and successful (-1.4 and -2.1 for wild-type and mutant, respectively). This result showed a nice correlation between the intermolecular energy of our solutions and the FCC between these solutions and the target (Figure 3).

DISCUSSION

The helicase enzyme, a motor protein, causes the unwinding of double-stranded nucleic acids along the 5′-3′ direction during biological processes such as recombination, replication, and repair (28). The SARS CoV-2 helicase interacts with

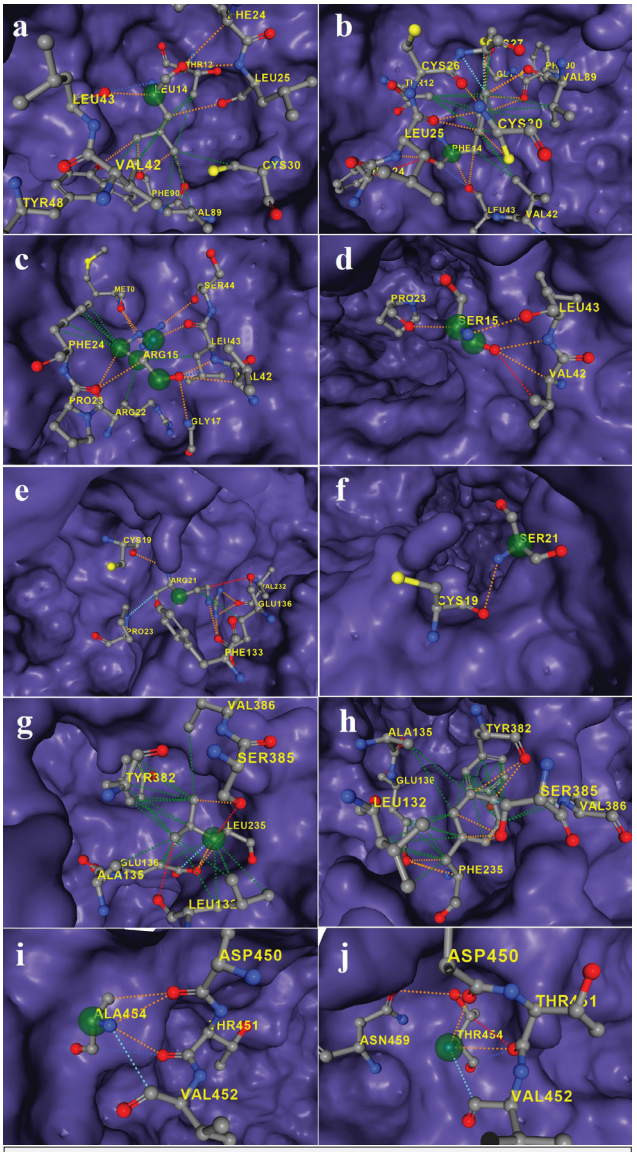

Figure 2. The change of inter-residual interaction in the tertiary structure of Helicase by mutations. Dashes indicates; red: hydrogen bond, orange: polar, green: hydrophobic, blue: Van der Walss. a: Leu14-wild-type, b: Phe14-mutant, c: Arg15-wild-type, d: Ser15-mutant, e: Arg21-wild-type, f: Ser21-mutant, g: Leu235-wild-type, h: Phe235-mutant, i: Ala454-wild-type, j: Phe454-mutant

human serine/threonine-protein kinase (TBK1). This interaction inhibits TBK1 phosphorylation and reduces interferon regulatory factor-3 phosphorylation by 75%, resulting in a reduction in the production of interferon-beta, one of the barriers to the viral invasion process (29,30). This study revealed that mutations in the SARS CoV-2 helicase, which is an important antiviral target, cause a decrease in substrate affinity and change in protein stability. The functional roles of proteins are formed by the dynamic movement and stability of their molecules (10,22). Mutations in the primary sequences of proteins change tertiary structure, stability, and function (31–33). A location-based evaluation of mutations is important in terms of the behavior of the virus in the cellular invasion process, the progression of the epidemic, and the specification of treatment options (34,35). The SARS CoV-2 has undergone thousands of mutations since the outbreak began, resulting in significant changes in its genome and protein structure (36,37). These changes manifested as various characteristics such as more virulence, increased affinity for the angiotensin converting enzyme-2 receptor, and faster host transition (38–40). The increase of the virus in the host cell is associated with an increased replication cycle and helicase activity. The opposite is also possible. Virus proteome rearrangements caused by mutations can increase or decrease virulence. Feroza et al. revealed two mutations with opposing effects on RNA-binding affinity with helicase (41). They reported that the Tyr541Cys substitution is a destabilizing mutation that increases molecular flexibility and leads to the reduced binding affinity for RNA and helicase, while the Phe504Leu substitution results in increased affinity (41). This study revealed that the Ala454Thr substitution in the 2A domain resulted in a decrease in protein stability (ΔΔG -0.73 kcal.mol^{-1}).

The interaction of active protein molecules and target nucleic acid sequence in the activation and regulation of replication and translation processes occurs with the contribution of special structural motifs such as zinc fingers (42,43). Zinc finger domain mutations result in alterations/weakening of target nucleic acid/protein and protein/protein interactions (44–46). According to the findings, three mutations (Leu14Phe, Arg15Ser, and Arg21Ser) in the zinc finger domain of the SARS CoV-2 helicase caused a decrease in protein stability (ΔΔG -0.99, -1.66, and -1.15 kcal.mol^{-1}, respectively) and a change in its conformation (Figure 2). Given the functional roles of the SARS CoV zinc finger structural motifs located in the N-terminus, it is clear that these mutations will result in significant changes in the functional properties of the helicase (47,48). The helicase-nucleic acid docking results indicated a decreased affinity of the SARS CoV-2 helicase (from -84.4 to -71.1 kcal.mol^{-1}). It is thought that the change in the bond interaction network of the residue in the zinc finger motif (^{26}Cys4), after the mutation affects the positive charge area, causes a weakening in the nucleic acid interaction (Figures 2a and b).

This study found that the Leu235Phe substitution located on the coil structure extending from the beta barrel formation to the nucleotide binding site between the 1A and 2A domains causes a decrease in protein stability (ΔΔG -0.54 kcal.mol^{-1}). This region of Leu235Phe substitution, located between the two domains responsible for nucleotide binding and hydrolysis, has been identified as a binding pocket for many candidate helicase inhibitors (49,50). Mutations are not only a threat to the functional roles of viral proteins, but also important for the validity of existing therapeutics. With mutations, the effectiveness of inhibitors can either increase or decrease.

Table 2. The change in helicase-nucleic acid interaction.

		Z-Score	DocSc	i-RMSD	Evdw	Eelec
1	**W**	-1.4	-84.4±1.4	16.8±4.2	-37.7±5.9	-322.8±19.7
	M	-2.1	-71.1±6.7	0.7±0.4	-40.9±13.3	-250.9±33.7
2	**W**	-1.4	-84.3±5.5	0.7±0.5	-36.3±5.0	-362.8±24.7
	M	-0.9	-57.0±2.5	7.7±0.7	-32.7±11.7	-180.4±47.7
3	**W**	-0.7	-71.2±9.0	7.4±1.4	-39.8±8.2	-245.5±47.5
	M	-0.8	-54.8±3.4	22.7±2.4	-26.9±3.8	-187.0±5.6
4	**W**	-0.6	-69.5±1.7	13.8±4.4	-31.0±3.7	-296.8±11.1
	M	0.2	-43.2±2.0	6.2±0.9	-20.1±6.3	-190.3±5.5
5	**W**	-0.1	-61.9±5.5	20.6±1.2	-34.8±4.4	-221.3±46.2
	M	0.3	-42.2±4.8	24.7±0.4	-43.1±8.4	-95.6±16.3
6	**W**	-0.1	-59.8±7.6	22.3±0.5	-32.0±3.9	-237.2±27.3
	M	0.4	-40.9±8.0	11.4±4.3	-19.3±8.1	-174.9±26.4
7	**W**	0.6	-49.3±5.1	24.8±3.8	-26.5±5.6	-185.9±23.0
	M	0.6	-38.1±7.2	23.9±0.5	-31.7±9.1	-92.2±14.0
8	**W**	0.9	-44.9±3.7	26.2±3.7	-34.2±5.7	-108.7±17.2
	M	1.1	-32.1±2.8	22.3±0.7	-17.4±4.5	-115.1±10.7
9	**W**	1.0	-43.1±1.3	24.8±3.8	-29.1±5.5	-150.4±28.4
	M	1.3	-29.5±5.1	28.9±2.0	-21.6±1.8	-54.3±24.1
10	**W**	1.7	-29.9±5.2	24.6±0.4	-23.2±4.2	-125.0±20.3
	M	-	-	-	-	-

W: wild, M: mutant, DocSc: docking score, i-RMSD: interface RMSD (from the overall lowest-energy structure), Evdw: Van der Waals energy, Eelec: electrostatic energy.

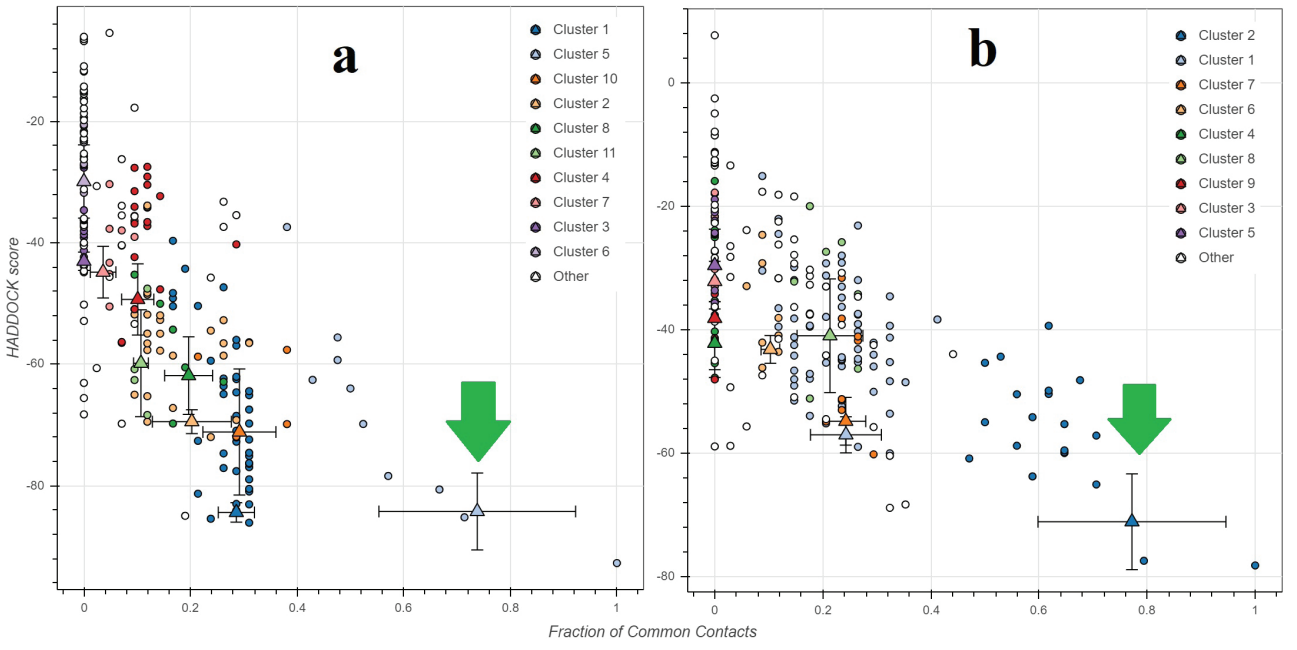

Figure 3. Evaluation of binding quality for wild-type helicase/nucleic acid and mutant helicase/nucleic acid complexes. a: wild-type helicase-nucleic acid complex, b: mutant helicase-nucleic acid complex.

CONCLUSION

The SARS CoV-2 nsp13 mutations decreased protein stability and nucleic acid affinity of helicase. The decreased helicase activity limits the replication and spread of SARS CoV-2 in the host cells. In China, which is the origin of the epidemic and the source of the isolates analyzed in this study, it is thought that successful epidemic control policies, as well as mutations in viral proteins in favor of the host, contributed to the decrease in the number of cases. The results provide important data on the development of potential antivirals and the effects of mutations on the functional behavior of viral proteins.

Acknowledgment: Genome data of Chinese isolates were obtained from the NCBI Virus database. Thanks to the NCBI Virus database for its open-source data sharing policy.

Peer Review: Externally peer-reviewed.

Conflict of Interest: Author declared no conflict of interest.

Financial Disclosure: Author declared no financial support.

REFERENCES

1. Singhal T. A Review of Coronavirus Disease-2019 (COVID-19). Indian J Pediatr 2020; 87: 281-6.
2. Zhou P, Yang X Lou, Wang XG, Hu B, Zhang L, Zhang W, et al. A pneumonia outbreak associated with a new coronavirus of probable bat origin. Nature 2020; 579: 270-3.
3. Worldometer. Coronavirus case report. WwwWorldometersInfo/Coronavirus 2022.
4. Wu F, Zhao S, Yu B, Chen YM, Wang W, Song ZG, et al. A new coronavirus associated with human respiratory disease in China. Nature 2020; 579: 265-9.
5. Zito Marino F, De Cristofaro T, Varriale M, Zannini G, Ronchi A, La Mantia E, et al. Variable levels of spike and ORF1ab RNA in post-mortem lung samples of SARS-CoV-2-positive subjects: comparison between ISH and RT-PCR. Virchows Arch 2022: 1-11.
6. Finkel Y, Mizrahi O, Nachshon A, Weingarten-Gabbay S, Morgenstern D, Yahalom-Ronen Y, et al. The coding capacity of SARS-CoV-2. Nature 2021; 589: 125-30.
7. Habtemariam S, Nabavi SF, Banach M, Berindan-Neagoe I, Sarkar K, Sil PC, et al. Should We Try SARS-CoV-2 Helicase Inhibitors for COVID-19 Therapy? Arch Med Res 2020; 51: 733-5.
8. Singleton MR, Dillingham MS, Wigley DB. Structure and mechanism of helicases and nucleic acid translocases. Annu Rev Biochem 2007; 76: 23-50.
9. Ahmad S, Waheed Y, Ismail S, Bhatti S, Abbasi SW, Muhammad K. Structure-based virtual screening identifies multiple stable binding sites at the RecA domains of SARS-CoV-2 helicase enzyme. Molecules 2021; 26: 1446.
10. Akbulut E. Mutations in the SARS CoV-2 spike protein may cause functional changes in the protein quaternary structure. Turkish J Biochem 2021; 46: 137-44.
11. Akbulut E. Comparative Genomic and Proteomic Analysis of SARS CoV-2 - with Potential Mutation Probabilities and Drug Targeting. Erzincan Univ J Sci Technol 2020; 13: 1187-97.
12. Zahradník J, Marciano S, Shemesh M, Zoler E, Harari D, Chiaravalli J, et al. SARS-CoV-2 variant prediction and antiviral drug design are enabled by RBD in vitro evolution. Nat Microbiol 2021; 6: 1188-98.
13. Katoh K. MAFFT: a novel method for rapid multiple sequence alignment based on fast Fourier transform. Nucleic Acids Res 2002; 30: 3059-66.
14. Mount DW. Using BLOSUM in sequence alignments. Cold Spring Harb Protoc 2008; 3: pdb-top39.
15. Jones DT, Taylor WR, Thornton JM. The rapid generation of mutation data matrices from protein sequences. Bioinformatics 1992; 8: 275-82.
16. Kumar S, Stecher G, Li M, Knyaz C, Tamura K. MEGA X: Molecular evolutionary genetics analysis across computing platforms. Mol Biol Evol 2018; 35: 1547-9.
17. Mirdita M, Ovchinnikov S, Steinegger M. ColabFold - Making protein folding accessible to all. BioRxiv 2021: 2021.08.15.456425.
18. Newman JA, Douangamath A, Yadzani S, Yosaatmadja Y, Aimon A, Brandão-Neto J, et al. Structure, mechanism and crystallographic fragment screening of the SARS-CoV-2 NSP13 helicase. Nat Commun 2021; 12.
19. Benkert P, Biasini M, Schwede T. Toward the estimation of the absolute quality of individual protein structure models. Bioinformatics 2011; 27: 343-50.
20. Rose AS, Bradley AR, Valasatava Y, Duarte JM, Prlic A, Rose PW. NGL viewer: Web-based molecular graphics for large complexes. Bioinformatics 2018; 34: 3755-8.
21. Xu J, Zhang Y. How significant is a protein structure similarity with TM-score = 0.5? Bioinformatics 2010; 26: 889-95.
22. Rodrigues CHM, Pires DEV, Ascher DB. DynaMut2: Assessing changes in stability and flexibility upon single and multiple point missense mutations. Protein Sci 2021; 30: 60-9.
23. Pires DEV, Ascher DB, Blundell TL. MCSM: Predicting the effects of mutations in proteins using graph-based signatures. Bioinformatics 2014; 30: 335-42.
24. Pires DEV, de Melo-Minardi RC, dos Santos MA, da Silveira CH, Santoro MM, Meira W. Cutoff Scanning Matrix (CSM): Structural classification and function prediction by protein inter-residue distance patterns. BMC Genomics, vol. 12, Springer; 2011, p. 1–11.
25. Pires DEV, De Melo-Minardi RC, Da Silveira CH, Campos FF, Meira W. ACSM: Noise-free graph-based signatures to large-scale receptor-based ligand prediction. Bioinformatics 2013; 29: 855-61.
26. Jubb HC, Higueruelo AP, Ochoa-Montaño B, Pitt WR, Ascher DB, Blundell TL. Arpeggio: A Web Server for Calculating and Visualising Interatomic Interactions in Protein Structures. J Mol Biol 2017; 429: 365-71.
27. Van Zundert GCP, Rodrigues JPGLM, Trellet M, Schmitz C, Kastritis PL, Karaca E, et al. The HADDOCK2.2 Web Server: User-Friendly Integrative Modeling of Biomolecular Complexes. J Mol Biol 2016; 428: 720-5.
28. Chen J, Malone B, Llewellyn E, Grasso M, Shelton PMM, Olinares PDB, et al. Structural Basis for Helicase-Polymerase Coupling in the SARS-CoV-2 Replication-Transcription Complex. Cell 2020; 182: 1560-1573.e13.
29. Leulier F, Parquet C, Pili-Floury S, Ryu JH, Caroff M, Lee WJ, et al. IK-Kepsilon and TBK1 are essential components of the IRF3 signaling pathway. Nat Immunol 2003; 4: 478-84. doi: 10.1038/ni922.
30. Xia H, Cao Z, Xie X, Zhang X, Chen JYC, Wang H, et al. Evasion of Type I Interferon by SARS-CoV-2. Cell Rep 2020; 33: 108234.
31. Nguyen TT, Chang SC, Evnouchidou I, York IA, Zikos C, Rock KL, et al. Structural basis for antigenic peptide precursor processing by the endoplasmic reticulum aminopeptidase ERAP1. Nat Struct Mol Biol 2011; 18: 604-13.
32. Wu S, Tian C, Liu P, Guo D, Zheng W, Huang X, et al. Effects of SARS-CoV-2 mutations on protein structures and intraviral protein–protein interactions. J Med Virol 2021; 93: 2132-40.

33. Akbulut E, Kar B. SARS CoV-2 nsp1 Mutasyonlarının Protein Yapıda Ortaya Çıkardığı Değişimler. Int J Pure Appl Sci 2020; 6: 68-76.
34. Farkas C, Fuentes-Villalobos F, Garrido JL, Haigh J, Barría MI. Insights on early mutational events in SARS-CoV-2 virus reveal founder effects across geographical regions. PeerJ 2020; 2020: e9255.
35. Garvin MR, T. Prates E, Pavicic M, Jones P, Amos BK, Geiger A, et al. Potentially adaptive SARS-CoV-2 mutations discovered with novel spatiotemporal and explainable AI models. Genome Biol 2020; 21: 1-26.
36. Alouane T, Laamarti M, Essabbar A, Hakmi M, Bouricha EM, Chemao-Elfihri MW, et al. Genomic diversity and hotspot mutations in 30,983 SARS-CoV-2 genomes: Moving toward a universal vaccine for the "confined virus"? Pathogens 2020; 9: 1-19.
37. Akbulut E. SARS CoV-2 Spike Glycoprotein Mutations and Changes in Protein Structure. Trak Univ J Nat Sci 2020; 22: 1-11.
38. Matyášek R, Kovařík A. Mutation patterns of human SARS-CoV-2 and bat RATG13 coronavirus genomes are strongly biased towards C>U transitions, indicating rapid evolution in their hosts. Genes (Basel) 2020; 11: 1-13.
39. Wang R, Hozumi Y, Zheng YH, Yin C, Wei GW. Host immune response driving SARS-CoV-2 evolution. Viruses 2020; 12: 1095.
40. Seyran M, Takayama K, Uversky VN, Lundstrom K, Palù G, Sherchan SP, et al. The structural basis of accelerated host cell entry by SARS-CoV-2†. FEBS J 2021; 288: 5010-20.
41. Feroza B, Banerjee AK, Tripathi PP, Ray U. Two mutations P/L and Y/C in SARS-CoV-2 helicase domain exist together and influence helicase RNA binding. BioRxiv 2020.
42. Jen J, Wang YC. Zinc finger proteins in cancer progression. J Biomed Sci 2016; 23: 1-9.
43. Iuchi S. Three classes of C2H2 zinc finger proteins. Cell Mol Life Sci 2001; 58: 625-35.
44. Filippova GN, Ulmer JE, Moore JM, Ward MD, Hu YJ, Neiman PE, et al. Tumor-associated zinc finger mutations in the CTCF transcription factor selectively alter its DNA-binding specificity. Cancer Res 2002; 62: 48-52.
45. Takaku M, Grimm SA, Roberts JD, Chrysovergis K, Bennett BD, Myers P, et al. GATA3 zinc finger 2 mutations reprogram the breast cancer transcriptional network. Nat Commun 2018; 9: 1-14.
46. Munro D, Ghersi D, Singh M. Two critical positions in zinc finger domains are heavily mutated in three human cancer types. PLoS Comput Biol 2018; 14: e1006290.
47. Ma J, Chen Y, Wu W, Chen Z. Structure and Function of N-Terminal Zinc Finger Domain of SARS-CoV-2 NSP2. Virol Sin 2021; 36: 1104-12.
48. Ma Y, Wu L, Shaw N, Gao Y, Wang J, Sun Y, et al. Structural basis and functional analysis of the SARS coronavirus nsp14-nsp10 complex. Proc Natl Acad Sci U S A 2015; 112: 9436-41.
49. Halder UC. Predicted antiviral drugs Darunavir, Amprenavir, Rimantadine and Saquinavir can potentially bind to neutralize SARS-CoV-2 conserved proteins. J Biol Res 2021; 28: 1-58.
50. Berta D, Badaoui M, Martino SA, Buigues PJ, Pisliakov A V., Elghobashi-Meinhardt N, et al. Modelling the active SARS-CoV-2 helicase complex as a basis for structure-based inhibitor design. Chem Sci 2021; 12: 13492-505.